Exciton in Halide Perovskite Nanoplatelets : Finite Confinement and Dielectric Effect in Effective Mass Approximation

Kaouther Tlili,[†,‡] Maria Chamarro,[‡] Kais Boujdaria,[†] and Christophe Testelin[*,‡]

[†] *Université de Carthage, Faculté des Sciences de Bizerte, LR01ES15 Laboratoire de Physique des Matériaux : Structure et Propriétés, 7021 Zarzouna, Bizerte, Tunisia*

[‡] *Sorbonne Université, CNRS, Institut des NanoSciences de Paris, F-75005, Paris, France*

E-mail: christophe.testelin@insp.upmc.fr

1 Bloch functions for the conduction band

The Bloch functions for the CB have p-symmetry with X_C, Y_C, and Z_C as the orbital basis. To characterize the p-conduction states, it is essential to consider the crystal field (CF) Hamiltonian, which accounts for the influence of tetragonal distortions on the cubic structure, as well as the spin-orbit coupling (SOC).

In the basis $\{|iX_C\uparrow\rangle, |iY_C\uparrow\rangle, |iZ_C\downarrow\rangle, |iX_C\downarrow\rangle, |iY_C\downarrow\rangle, |iZ_C\uparrow\rangle\}$, where $\uparrow$ ($\downarrow$) indicates the spin-up (spin-down) state, the effective Hamiltonian $H(0)$ for the p conduction states is represented by the matrix:

$$H(0) = \begin{pmatrix} M_1 & 0 \\ 0 & M_2 \end{pmatrix} \tag{1}$$

where

$$M_1 = \begin{pmatrix} E_C^{(0)} + \frac{T_0}{3} & -i\frac{\Delta_{SO}}{3} & \frac{\Delta_{SO}}{3} \\ i\frac{\Delta_{SO}}{3} & E_C^{(0)} + \frac{T_0}{3} & -i\frac{\Delta_{SO}}{3} \\ \frac{\Delta_{SO}}{3} & i\frac{\Delta_{SO}}{3} & E_C^{(0)} - \frac{2T_0}{3} \end{pmatrix}, M_2 = \begin{pmatrix} E_C^{(0)} + \frac{T_0}{3} & i\frac{\Delta_{SO}}{3} & -\frac{\Delta_{SO}}{3} \\ -i\frac{\Delta_{SO}}{3} & E_C^{(0)} + \frac{T_0}{3} & -i\frac{\Delta_{SO}}{3} \\ -\frac{\Delta_{SO}}{3} & i\frac{\Delta_{SO}}{3} & E_C^{(0)} - \frac{2T_0}{3} \end{pmatrix} \quad (2)$$

Here, $E_C^{(0)}$ is the CB edge energy without the bulk tetragonal CF and SOC, T_0 is the bulk tetragonal crystal field parameter, and Δ_{SO} is the spin-orbit coupling parameter.

The eigenenergies and eigenstates of $H(0)$ are:

- $E^{(0)}_{|1/2,\pm 1/2\rangle_C} = E_C^{(0)} - \frac{\Delta_{SO}+T_0}{6} - \frac{1}{2}\sqrt{\Delta_{SO}^2 - \frac{2}{3}\Delta_{SO}T_0 + T_0^2}$

which is associated to the eigenstates:

$$\begin{cases} |1/2,1/2\rangle_C = i\left[\left| -\dfrac{\cos\theta}{\sqrt{2}}(X_C + iY_C)\downarrow - \sin\theta Z_C\uparrow \right\rangle\right] \\ |1/2,-1/2\rangle_C = i\left[\left|\dfrac{\cos\theta}{\sqrt{2}}(X_C - iY_C)\uparrow - \sin\theta Z_C\downarrow \right\rangle\right] \end{cases} \quad (3)$$

- $E^{(0)}_{|3/2,\pm 1/2\rangle_C} = E_C^{(0)} - \frac{\Delta_{SO}+T_0}{6} + \frac{1}{2}\sqrt{\Delta_{SO}^2 - \frac{2}{3}\Delta_{SO}T_0 + T_0^2}$

with corresponding eigenstates:

$$\begin{cases} |3/2,1/2\rangle_C = i\left[\left| -\dfrac{\sin\theta}{\sqrt{2}}(X_C + iY_C)\downarrow + \cos\theta Z_C\uparrow \right\rangle\right] \\ |3/2,-1/2\rangle_C = i\left[\left|\dfrac{\sin\theta}{\sqrt{2}}(X_C - iY_C)\uparrow + \cos\theta Z_C\downarrow \right\rangle\right] \end{cases} \quad (4)$$

- $E^{(0)}_{|3/2,\pm 3/2\rangle_C} = E_C^{(0)} + \frac{\Delta_{SO}+T_O}{3}$

with corresponding eigenstates:

$$\begin{cases} |3/2,3/2\rangle_C = i\left[\left| -\frac{1}{\sqrt{2}}(X_C + iY_C)\uparrow \right\rangle\right] \\ |3/2,-3/2\rangle_C = i\left[\left|\frac{1}{\sqrt{2}}(X_C - iY_C)\downarrow \right\rangle\right] \end{cases} \tag{5}$$

where $\tan(2\theta) = \frac{2\sqrt{2}\Delta_{SO}}{\Delta_{SO}-3T_0}$ (with $0 < \theta < \pi/2$).

2 Coulomb interactions and self-energy potentials

As explained in section 2.3, the effect of the dielectric-constant difference between the well and barrier layers is included in the Coulomb interactions and self-energy. In this section, we give the expressions of these potentials, for carrier wavefunction delocalized in NPL barriers. In Figure. 2 , the well layer is denoted as C, while the barrier layers on the left side and right side are denoted as L and R, respectively.

The Coulomb potential of an electron in region A and a hole in region B will be represented as $V_C^{AB}(r_e, r_h)$. Nine configurations corresponding to different spatial arrangements are described as follows:

- z_e *and* $z_h \in C$: $|z_e|$ and $|z_h| \leq \frac{L_z}{2}$

$$V_C^{CC}(r_e, r_h) = -\frac{1}{4\pi\epsilon_0} \times \sum_{n=-\infty}^{+\infty} \frac{q_n e^2}{\epsilon_1 \left[(\rho_e - \rho_h)^2 + [z_e - (-1)^n z_h - nL_z]^2\right]^{\frac{1}{2}}} \tag{6}$$

- $z_e \in L$ *and* $z_h \in C$: $z_e < \frac{-L_z}{2}$ *and* $|z_h| \leq \frac{L_z}{2}$

$$V_C^{LC}(r_e, r_h) = -\frac{1}{4\pi\epsilon_0}\frac{2\epsilon_1}{\epsilon_1+\epsilon_2} \times \sum_{n=0}^{+\infty} \frac{q_n e^2}{\epsilon_1 \left[(\rho_e - \rho_h)^2 + [z_e - (-1)^n z_h - nL_z]^2\right]^{\frac{1}{2}}} \tag{7}$$

- $z_e \in R \; and \; z_h \in C : \; z_e > \frac{L_z}{2} \; and \; |z_h| \leq \frac{L_z}{2}$

$$V_C^{RC}(r_e, r_h) \;\; = \;\; -\frac{1}{4\pi\epsilon_0}\frac{2\epsilon_1}{\epsilon_1+\epsilon_2} \times \sum_{n=0}^{+\infty} \frac{q_n e^2}{\epsilon_1 \Bigg[(\rho_e-\rho_h)^2 + [z_e - (-1)^n z_h + nL_z]^2\Bigg]^{\frac{1}{2}}} \quad (8)$$

- $z_e \; and \; z_h \in L : \; z_e$ and $z_h < \frac{-L_z}{2}$

$$V_C^{LL}(r_e, r_h) = -\frac{1}{4\pi\epsilon_0}\left(\frac{2\epsilon_1}{\epsilon_1+\epsilon_2}\right)^2 \times \sum_{n=0}^{+\infty} \frac{q_{2n+1} e^2}{\epsilon_1 \Bigg[(\rho_e-\rho_h)^2 + [z_e + z_h - (2n+1)L_z]^2\Bigg]^{\frac{1}{2}}}$$
$$- \frac{1}{4\pi\epsilon_0}\frac{e^2}{\epsilon_2 \Bigg[(\rho_e-\rho_h)^2 + (z_e - z_h)^2\Bigg]^{\frac{1}{2}}} + \frac{1}{4\pi\epsilon_0}\frac{q_1 e^2}{\epsilon_2 \Bigg[(\rho_e-\rho_h)^2 + (z_e + z_h + L_z)^2\Bigg]^{\frac{1}{2}}} \quad (9)$$

- $z_e \in C \; and \; z_h \in L : \; |z_e| \leq \frac{L_z}{2} \; and \; z_h < \frac{-L_z}{2}$

$$V_C^{CL}(r_e, r_h) \;\; = \;\; -\frac{1}{4\pi\epsilon_0}\frac{2\epsilon_1}{\epsilon_1+\epsilon_2} \times \sum_{n=0}^{+\infty} \frac{q_n e^2}{\epsilon_1 \Bigg[(\rho_e-\rho_h)^2 + [z_h - (-1)^n z_e - nL_z]^2\Bigg]^{\frac{1}{2}}} \quad (10)$$

- $z_e \in R \; and \; z_h \in L : \; z_e > \frac{L_z}{2} \; and \; z_h < \frac{-L_z}{2}$

$$V_C^{RL}(r_e, r_h) \;\; = \;\; -\frac{1}{4\pi\epsilon_0}\left(\frac{2\epsilon_1}{\epsilon_1+\epsilon_2}\right)^2 \times \sum_{n=0}^{+\infty} \frac{q_{2n} e^2}{\epsilon_1 \Bigg[(\rho_e-\rho_h)^2 + [z_e - z_h + 2nL_z]^2\Bigg]^{\frac{1}{2}}} \quad (11)$$

- $z_e \in L \; and \; z_h \in R : \; z_e < \frac{-L_z}{2} \; and \; z_h > \frac{L_z}{2}$

$$V_C^{LR}(r_e, r_h) \;\; = \;\; -\frac{1}{4\pi\epsilon_0}\left(\frac{2\epsilon_1}{\epsilon_1+\epsilon_2}\right)^2 \times \sum_{n=0}^{+\infty} \frac{q_{2n} e^2}{\epsilon_1 \Bigg[(\rho_e-\rho_h)^2 + [z_e - z_h - 2nL_z]^2\Bigg]^{\frac{1}{2}}} \quad (12)$$

- $z_e \in C \; and \; z_h \in R : \; |z_e| \leq \frac{L_z}{2} \; and \; z_h > \frac{L_z}{2}$

$$V_C^{CR}(r_e, r_h) \;=\; -\frac{1}{4\pi\epsilon_0}\frac{2\epsilon_1}{\epsilon_1+\epsilon_2} \times \sum_{n=0}^{+\infty} \frac{q_n e^2}{\epsilon_1\left[(\rho_e-\rho_h)^2+[z_h-(-1)^n z_e+nL_z]^2\right]^{\frac{1}{2}}} \quad (13)$$

- $z_e \; and \; z_h \in R : \; z_e \text{ and } z_h > \frac{L_z}{2}$

$$V_C^{RR}(r_e, r_h) = -\frac{1}{4\pi\epsilon_0}\left(\frac{2\epsilon_1}{\epsilon_1+\epsilon_2}\right)^2 \times \sum_{n=0}^{+\infty} \frac{q_{2n+1} e^2}{\epsilon_1\left[(\rho_e-\rho_h)^2+[z_e+z_h+(2n+1)L_z]^2\right]^{\frac{1}{2}}}$$
$$-\frac{1}{4\pi\epsilon_0}\frac{e^2}{\epsilon_2\left[(\rho_e-\rho_h)^2+(z_e-z_h)^2\right]^{\frac{1}{2}}} + \frac{1}{4\pi\epsilon_0}\frac{q_1 e^2}{\epsilon_2\left[(\rho_e-\rho_h)^2+(z_e+z_h-L_z)^2\right]^{\frac{1}{2}}} \quad (14)$$

with $q_n = \left(\frac{\epsilon_1-\epsilon_2}{\epsilon_1+\epsilon_2}\right)^{|n|} = \eta^{|n|}$

Concerning the self-energy potential, valid expressions exist for both types of charge carriers, leading to three possible configurations for each charge carrier. The self-energy potentials are presented as follows, where z represents the coordinate for either the electron or the hole:

- $z \in C : \; |z| \leq \frac{L_z}{2}$

$$V_{self}^{C}(r) \quad = \quad \frac{1}{4\pi\epsilon_0} \;\times\; \left[\frac{e^2}{2\epsilon_1 L_z}\ln(\frac{1}{1-\eta}) \;+\; \sum_{p=0}^{+\infty} \frac{q_1^{2p+1}(2p+1)L_z e^2}{\epsilon_1\left[[(2p+1)L_z]^2-4z^2\right]}\right] \quad (15)$$

- $z \in L : \; z \leq \frac{-L_z}{2}$

$$V_{self}^{L}(r) \;=\; \frac{1}{4\pi\epsilon_0} \times \left[-\frac{q_1 e^2}{2\epsilon_2|2z+L_z|} + \frac{2\epsilon_1}{\epsilon_1+\epsilon_2}\sum_{n=0}^{+\infty} \frac{q_{2n+1} e^2}{(\epsilon_1+\epsilon_2)\left|2z-(2n+1)L_z\right|}\right] \quad (16)$$

- $z \in R : z \geq \frac{L_z}{2}$

$$V^R_{self}(r) = \frac{1}{4\pi\epsilon_0} \times \left[-\frac{q_1 e^2}{2\epsilon_2 |2z - L_z|} + \frac{2\epsilon_1}{\epsilon_1 + \epsilon_2} \sum_{n=0}^{+\infty} \frac{q_{2n+1} e^2}{(\epsilon_1 + \epsilon_2) \left| 2z + (2n+1)L_z \right|} \right] \quad (17)$$

3 Carrier penetration lengths in the organic barrier

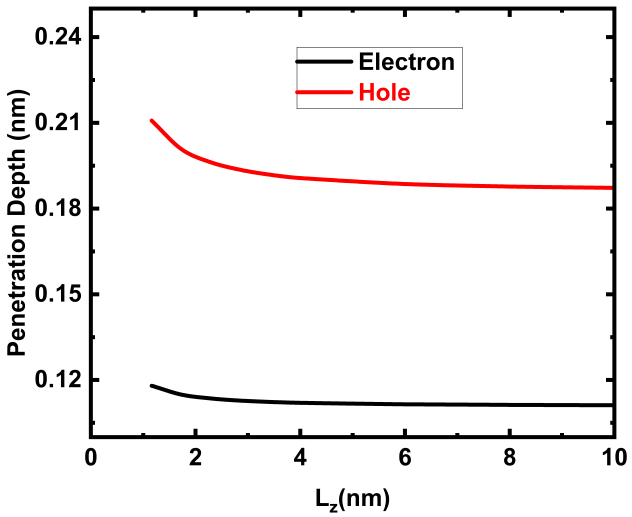

Figure S1: Penetration length versus NPL thickness for electron and hole, in $CsPbBr_3$ NPLs (black and red curves)

From the derivation described in Section 2.5, one deduced κ_p ($p = e, h$), the decay rate of the electron/hole WF. One can then define a carrier penetration length $\ell_p = \kappa_p^{-1}$. The dependence of ℓ_p with the NPL thickness is shown in Figure S1. Except for a small increase, for L_z = 2-4 ML, the penetration lengths are constant, of the order of 0.12 and 0.19 nm, for electron and hole, very comparable to DFT calculations.[1] Both carriers having close effective masses, the hole has a larger penetration length than the electron, due to a smaller band offset.

References

(1) Khabibulli, A.; Efros, A.; Erwin, S. "Dielectric Effects on the Electronic Properties of Colloidal Quantum Dots". *Nanoscale* **2020**, *12*, 23028–23035.